Military Technical College
Kobry El-kobbah,
Cairo, Egypt

5th International Conference
on Electrical Engineering
ICEENG 2006

Performance Analysis of Strapdown Inertial Navigation Algorithms

Ahmed Azouz, Ezz Eldin Farouk and Ahmed El-Said

ABSTRACT

In this work the theory of strapdown inertial navigation is introduced. The strapdown inertial navigation algorithms using Euler angles, direction cosines, and quaternions methods are derived. Reference flow charts of strapdown INS algorithms for attitude calculation based on Euler angles, direction cosines, and quaternions methods are derived.Simulation examples applied on the navigation of Aerosonde UAV. Simulation results are analyzed to explore the differences between the different algorithms to conclude the most reliable algorithm of strapdown inertial navigation algorithms.

KEYWORDS

INS	Inertial Navigation System
IMU	Inertial Measurement Unit
RMS	Root Mean Square
GPS	Global Positioning Systems
DCM	Direction Cosines Matrix
MEMS	Micro-Electro-Mechanical Systems

NOMENCLATURE

ω_x	Angular velocity in x axis in body frame in rad/sec
ω_y	Angular velocity in y axis in body frame in rad/sec
ω_z	Angular velocity in z axis in body frame in rad/sec
a_x	acceleration in x axis in body frame in m/sec^2
a_Y	acceleration in y axis in body frame in m/sec^2
a_z	acceleration in z axis in body frame in m/sec^2
F_N	acceleration in x axis (north) in navigation frame in m/sec^2
F_E	acceleration in y axis (east) in navigation frame in m/sec^2
F_D	acceleration in z axis (down) in navigation frame in m/sec^2
v_N	velocity in x axis (north) in navigation frame in m/sec

v_E	velocity in y axis (east) in navigation frame in m/sec
v_D	velocity in z axis (down) in navigation frame in m/sec
φ	Position latitude in rad
λ	Position longitude in rad
h	Position altitude in meter
C_n^b	Transformation matrix from navigation frame to body frame
C_b^n	Transformation matrix from body frame to navigation frame
g^n	Gravitational acceleration in navigation frame in m/sec^2
ω_e	Angular velocity of earth in rad/sec
ϕ	Attitude roll in rad
θ	Attitude pitch in rad
ψ	Attitude yaw in rad

1- Introduction

In recent years a worldwide development in strapdown INS algorithms with new approaches to accommodate modern computer technologies are developed [1-10]. These efforts are mainly for high performance INS, (strategic-grade and navigation grade), are analyzed based on technology developments. In strapdown INS the sensors (gyros and accelerometers) are rigidly attached (i.e., strapdown) to the body of the vehicle and hence the quantities that they measure (angular velocity, specific force) are in body-fixed coordinates. Determination of the position of body, however, requires knowledge of the specific force component in the navigation coordinates [5]. The transformation from body coordinates to inertial coordinates requires accurate knowledge of the vehicle attitude.

In this paper the INS dynamics equations of both navigation-grade and lower grade based on IMU s are derived. In section-2 various coordinate frames are defined. In section-3 navigation equations are developed on the basis of the navigation frame which is widely used in the navigation society. In section-4 the attitude of the vehicle relative to the navigation reference frame can be described by variables, the most popular are Euler angles, direction cosines, and quaternions. In section-5 Simulation to test algorithm of INS and RMS error analysis is explored to show the performance strength of each algorithm.

2 Navigation Coordinate Frames

Coordinate systems are investigated to develop the navigation equations and to get the dynamic motion of an aircraft. Aircraft navigation systems determine the navigation equations to determine position, velocity, and attitude information with respect to specific frames. The coordinates presented here are used in navigation with GPS and /or INS. The choice of the application frame will depend, to a large extent, on the mission requirement, each of implementation, computer storage and speed and navigation equation solution complicity [6].

2.1 Inertial Frame (I-Frame): (x^i, y^i, z^i)

The inertial frame has its origin at the center of the Earth and axes which are non-rotating with respect to the fixed stars with its z-axis parallel to the spin axis of the Earth x-axis pointing towards the mean vernal equinox and y-axis completing a right handed orthogonal frame as shown in Fig.1. The vernal equinox is the ascending node between the celestial equator and the ecliptic. So the right ascension system is used as the inertial frame in practice since it closely approximates an inertial frame [6].

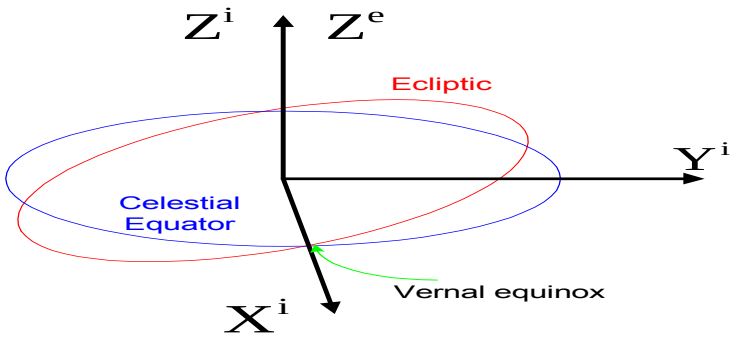

Fig.1: Inertial frame

2.2 Earth Centered, Earth Fixed Frame (E-Frame): (x^e, y^e, z^e)

The Earth frame has its origin at the center of mass of the Earth and axes which are fixed with respect to the Earth. Their x-axis point towards the mean meridian of Greenwich z-axis is parallel to the mean spin axis of the Earth and [6] y-axis completes a right-handed orthogonal frame shown in Fig.2.

2.3 Navigation Frame (N-Frame): (x^n, y^n, z^n)

The navigation frame (n-frame) is a local geodetic frame which has its origin coinciding with that of the sensor frame and axis with x-axis pointing towards geodetic north z-axis orthogonal to the reference ellipsoid pointing down and y-axis completing a right-handed orthogonal frame i.e. the north east-down (NED) system as shown in Fig.2. The benefit of the east north-up (ENU) system is that altitude increases in the upward. The advantage of NED system is that the direction of a right turn is in the positive direction with respect to a downward axis [3]. Further NED system is prevalent and therefore more research results can be found and incorporated into one's own directly.

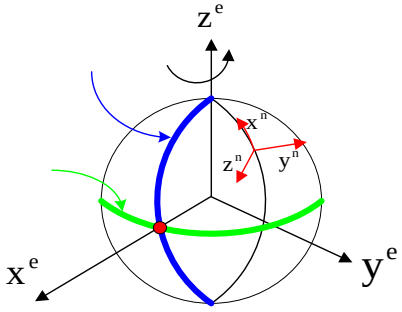

Fig.2: Earth centered, earth fixed frame and the navigation frame

2.4 Body Frame (B-Frame): (x^b, y^b, z^b)

The body frame is an orthogonal axis set which is aligned with the roll pitch and heading axes of a vehicle i.e. forward-transversal-down. x-axis (roll) in the nominal direction of motion of vehicle, y-axis (pitch) orthogonal out the right hand side, and z-axis (yaw) completing a right-handed orthogonal frame such that turning to right is positive [6]. As shown in Fig.3.

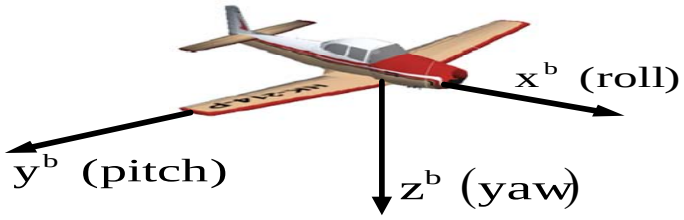

Fig.3: body frame

3 Inertial Navigation Equations

The navigation equations for the inertial device must be derived from an inertial frame. This is generally taken as the inertial frame, which is located at the center of the earth and fixed in space, i.e. it does not rotate with the earth. For referencing purposes, the navigation equations are usually put into the NED frame since the geographical representation of NED is the most intuitive.

3.1 The Position in the N-Frame

The position in the n-frame is expressed by curvilinear coordinates [9]:

$$r^n = (\varphi \quad \lambda \quad h)^T \tag{1}$$

and the velocities in the n–frame are defined by

$$\dot{v}^n = \begin{pmatrix} \dot{v}_N \\ \dot{v}_E \\ \dot{v}_D \end{pmatrix} = \begin{pmatrix} M+h & 0 & 0 \\ 0 & (N+h)\cos(\varphi) & 0 \\ 0 & 0 & -1 \end{pmatrix} \begin{pmatrix} \dot{\varphi} \\ \dot{\lambda} \\ \dot{h} \end{pmatrix} \tag{2}$$

Hence the time derivative of the coordinates can be written as

$$\dot{r}^n = \begin{pmatrix} \dot{\varphi} \\ \dot{\lambda} \\ \dot{h} \end{pmatrix} = \begin{pmatrix} \frac{1}{M+h} & 0 & 0 \\ 0 & \frac{1}{(N+h)\cos(\varphi)} & 0 \\ 0 & 0 & -1 \end{pmatrix} \begin{pmatrix} v_N \\ v_E \\ v_D \end{pmatrix} = D^{-1} v^n \tag{3}$$

where

$M = \dfrac{r_e\,(1-E^2)}{(1-E^2\sin^2\varphi)^{3/2}}$ the meridian radius, in meters.

$N = \dfrac{r_e}{(1-E^2\sin^2\varphi)^{1/2}}$ the normal radius, in meters.

3.2 Velocity Dynamics Equations in the N-Frame

To get the velocity dynamics equations we start with [9]:

$$v^n = C_e^n \dot{r}^e \tag{4}$$

The derivation of velocity equation in navigation frame is given in [9].

$$\dot{v}^n = C_b^n\left(f^b\right) - (2\Omega_{ie}^n + \Omega_{en}^n)\, v^n - g^n \quad (5)$$

The equation of velocity of navigation frame (velocity north east down)

$$\dot{v}_N = -(\dot{\lambda} + 2\omega_e)\sin(\varphi)\, v_E + \dot{\varphi}\, v_D + F_N \quad (6)$$

$$\dot{v}_E = (\dot{\lambda} + 2\omega_e)\sin(\varphi)\, v_N + (\dot{\lambda} + 2\omega_e)\cos(\varphi)\, v_D + F_E \quad (7)$$

$$\dot{v}_D = -\dot{\varphi}\, v_N - (\dot{\lambda} + 2\omega_e)\cos(\varphi)\, v_E + F_D + g_n \quad (8)$$

$$F = \begin{bmatrix} F_N \\ F_E \\ F_D \end{bmatrix} = C_b^n . \begin{bmatrix} a_X \\ a_Y \\ a_Z \end{bmatrix} \quad (9)$$

Where

$f = [\, a_x \quad a_y \quad a_z \,]^T$ measurement accelerometer in body frame.

$F = [\, F_N \quad F_E \quad F_D \,]^T$ specific force in navigation frame

4 The Attitude Dynamics

The attitude of the vehicle with respect to designated reference frame (navigation frame) may be set of numbers in computer within the vehicle. The stored attitude is updated as the vehicle rotates using the measurements of turn rate provided by the gyroscopes.

4.1 The Attitude Dynamics Using Euler

The angles of rotation about each of these axes are called Euler angles. Euler angles (roll, pitch, and yaw) are a set of three ordered rotations necessary to bring the reference axes of one system (body) into coincidence with reference axes of the other (navigation). The attitude of vehicle body with respect to location coordinates can be specified in terms of rotation about the vehicle roll, pitch, and yaw, starting with these axes aligned with NED coordinates. It is always necessary to specify the order of rotations when specifying Euler angles

1-Roll: Rotation through the roll angle (ϕ) about the vehicle x^b axis to bring the vehicle attitude to the specified orientation [3].

2-Pitch: Rotation through the pitch angle (θ) about the vehicle y^b axis to bring the vehicle x^b axis to its intended elevation. Elevation is measured positive upward from the location plan.

3-Yaw/Heading: Rotate through the yaw angle (ψ) about the vehicle z^b axis to the intended azimuth (heading) of the vehicle x^b axis. Azimuth is measured clockwise (east) from north.

Euler angles are used to define a coordinate transformation from body frame to navigation frame [3] as given in the following equations.

$$C_n^b = R_x(\phi) R_y(\theta) R_z(\psi) \quad (10)$$

$$C_b^n = \left(C_n^b\right)^T = R_z(-\psi) R_y(-\theta)\, R_y(-\phi) \quad (11)$$

$$C_b^n = \begin{pmatrix} \cos\psi & -\sin\psi & 0 \\ \sin\psi & \cos\psi & 0 \\ 0 & 0 & 1 \end{pmatrix} \begin{pmatrix} \cos\theta & 0 & \sin\theta \\ 0 & 1 & 0 \\ -\sin\theta & 0 & \cos\theta \end{pmatrix} \begin{pmatrix} 1 & 0 & 0 \\ 0 & \cos\phi & -\sin\phi \\ 0 & \sin\phi & \cos\phi \end{pmatrix}$$

$$= \begin{pmatrix} \cos\theta\cos\psi & -\cos\phi\sin\psi+\sin\phi\sin\theta\cos\psi & \sin\phi\sin\psi+\cos\phi\sin\theta\cos\psi \\ \cos\theta\sin\psi & \cos\phi\cos\psi+\sin\phi\sin\theta\sin\psi & -\sin\phi\cos\psi+\cos\phi\sin\theta\sin\psi \\ -\sin\theta & \sin\phi\cos\theta & \cos\phi\cos\theta \end{pmatrix} \quad (12)$$

The Euler angles can also be determined from the DCM C_b^n by the following equations [7].

$$\theta = \sin^{-1}[-C_n^b(1,3)] \quad (13)$$

$$\dot{\theta} = \left(\omega_y \sin\phi - \omega_z \cos\phi\right) \quad (14)$$

$$\phi = \sin^{-1}\left[\frac{C_n^b(2,3)}{\cos(\theta)}\right] \quad (15)$$

$$\dot{\phi} = \omega_x + \tan\theta\left(\omega_y \sin\phi + \omega_z \cos\phi\right) \quad (16)$$

$$\psi = \sin^{-1}\left[\frac{C_n^b(1,2)}{\cos(\theta)}\right] \quad (17)$$

$$\dot{\psi} = \frac{\left(\omega_y \sin\phi + \omega_z \cos\phi\right)}{\cos\theta} \quad (18)$$

The equations (3), (5), (14), (16), and (18) can be written in one equation form as given in equation (19).

$$\begin{pmatrix} \dot{r}^n \\ \dot{v}^n \\ \dot{\phi} \\ \dot{\theta} \\ \dot{\psi} \end{pmatrix} = \begin{pmatrix} D^{-1}v^n \\ C_b^n f^b - (2\omega_{ie}^n + \omega_{en}^n)\times v^n + g^n \\ \omega_x + \tan\theta\left(\omega_y \sin\phi + \omega_z \cos\phi\right) \\ \left(\omega_y \sin\phi - \omega_z \cos\phi\right) \\ \dfrac{\left(\omega_y \sin\phi + \omega_z \cos\phi\right)}{\cos\theta} \end{pmatrix} \quad (19)$$

The flow chart, shown in Fig.4, indicates the details of strapdown INS algorithm for attitude calculation based on Euler angles.

4.2 The Attitude Dynamics Using Direction Cosines

The direction cosine matrix, denoted here by the symbol C_n^b, is a 3 x 3 matrix, the columns of which represent unit vectors in navigation axes projected along the body axes. C_n^b is written here in component form as follows:

$$C_n^b = \begin{pmatrix} c_{11} & c_{12} & c_{13} \\ c_{21} & c_{22} & c_{23} \\ c_{31} & c_{32} & c_{33} \end{pmatrix} \quad (20)$$

The element c_{ij} equal to the cosine of the angle between ith axis of the reference frame and the jth axis of the body frame.

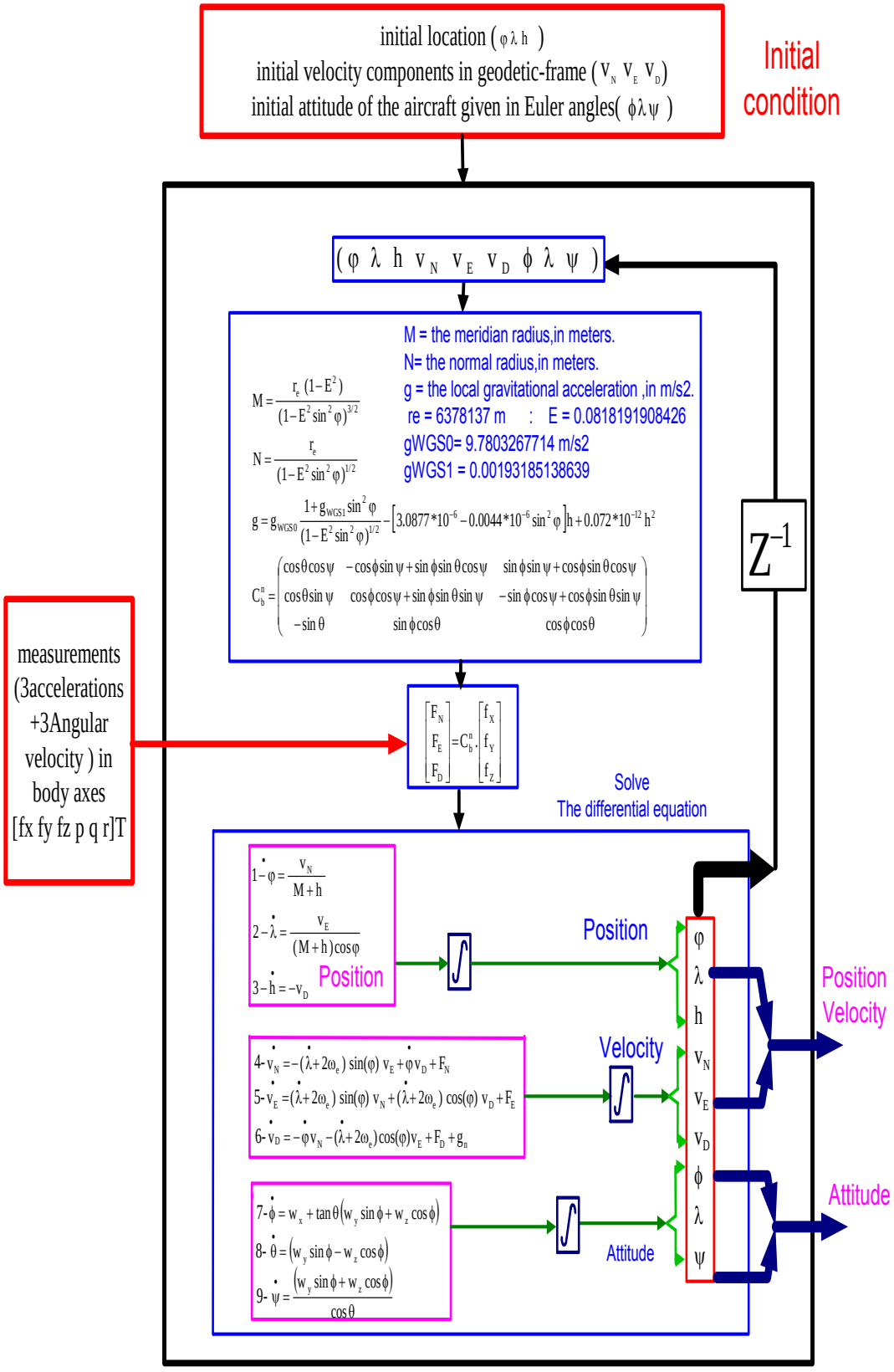

Fig.4: The flow chart of strapdown INS algorithm for attitude calculation based on Euler angles.

4.2.1 The Attitude Dynamics Using Direction Cosines

The rate of change of C_b^n with time is given by:

$$\dot{C}_b^n = \lim_{\delta t \to 0} \frac{\delta C_b^n}{\delta t} = \lim_{\delta t \to 0} \frac{C_b^n(t+\delta t) - C_b^n(t)}{\delta t} \quad (21)$$

where $C_b^n(t)$ and $C_b^n(t+\delta t)$ represent the direction cosine matrix at times t and $t+\delta t$ respectively. $C_b^n(t+\delta t)$ can be written as the product of two matrices as follows:

$$C_b^n(t+\delta t) = C_b^n(t)\ A(t) \quad (22)$$

where A(t) is a direction cosine matrix which relates the body frame at time t to the body frame at time $t+\delta t$. For small angle rotations, A(t) may be written as follows:

$$A(t) = [\ I + \delta\Psi\ ] \quad (23)$$

Where I is a 3×3 identity matrix and

$$\delta\Psi = \begin{pmatrix} 0 & -\delta\psi & \delta\theta \\ \delta\psi & 0 & \delta\phi \\ -\delta\theta & \delta\phi & 0 \end{pmatrix} \quad (24)$$

In which $\delta\phi, \delta\theta$ and $\delta\psi$ are small rotation angles through which the body frame has rotation over the time interval δt about its roll, pitch, and yaw axes respectively. In the limit as δt approaches zero, small angle approximations are valid and the order of the rotation becomes unimportant.

Substituting equation (23) and (22) in (21)

$$\dot{C}_b^n = C_b^n \lim_{\delta t \to 0} \frac{\delta\Psi}{\delta t} \quad (25)$$

In the limit as $\delta t \to 0$, $\delta\Psi/\delta t$ is the skew symmetric form of the angular rate vector $\omega_{nb}^b = (\omega_x\ \omega_y\ \omega_z)^T$, which represents the turn rate of body frame with respect to the navigation frame expressed in body axes, i.e.

$$\lim_{\delta t \to 0} \frac{\delta\Psi}{\delta t} = \Omega_{nb}^b \quad (26)$$

Substituting equation (26) in (25)

$$\dot{C}_b^n = C_b^n\ \Omega_{nb}^b = \begin{pmatrix} c_{11} & c_{12} & c_{13} \\ c_{21} & c_{22} & c_{23} \\ c_{31} & c_{32} & c_{33} \end{pmatrix} \begin{pmatrix} 0 & -\omega_z & \omega_y \\ \omega_z & 0 & \omega_x \\ -\omega_y & \omega_x & 0 \end{pmatrix} \quad (27)$$

An equation of the form as (27) may be solved by a computer in strapdown INS to keep track of body attitude with respect to navigation frame detail in [7] and [8].

The equations (3), (5), and (27) can be written in one equation form as given in equation (28).

$$\begin{pmatrix} \dot{r}^n \\ \dot{v}^n \\ \dot{C}_b^n \end{pmatrix} = \begin{pmatrix} D^{-1} v^n \\ C_b^n f^b - (2\omega_{ie}^n + \omega_{en}^n) \times v^n + g^n \\ C_b^n\ \Omega_{nb}^b \end{pmatrix} \quad (28)$$

The flow chart, shown in Fig.5, indicates the details of strapdown INS algorithm for attitude calculation based on direction cosines.

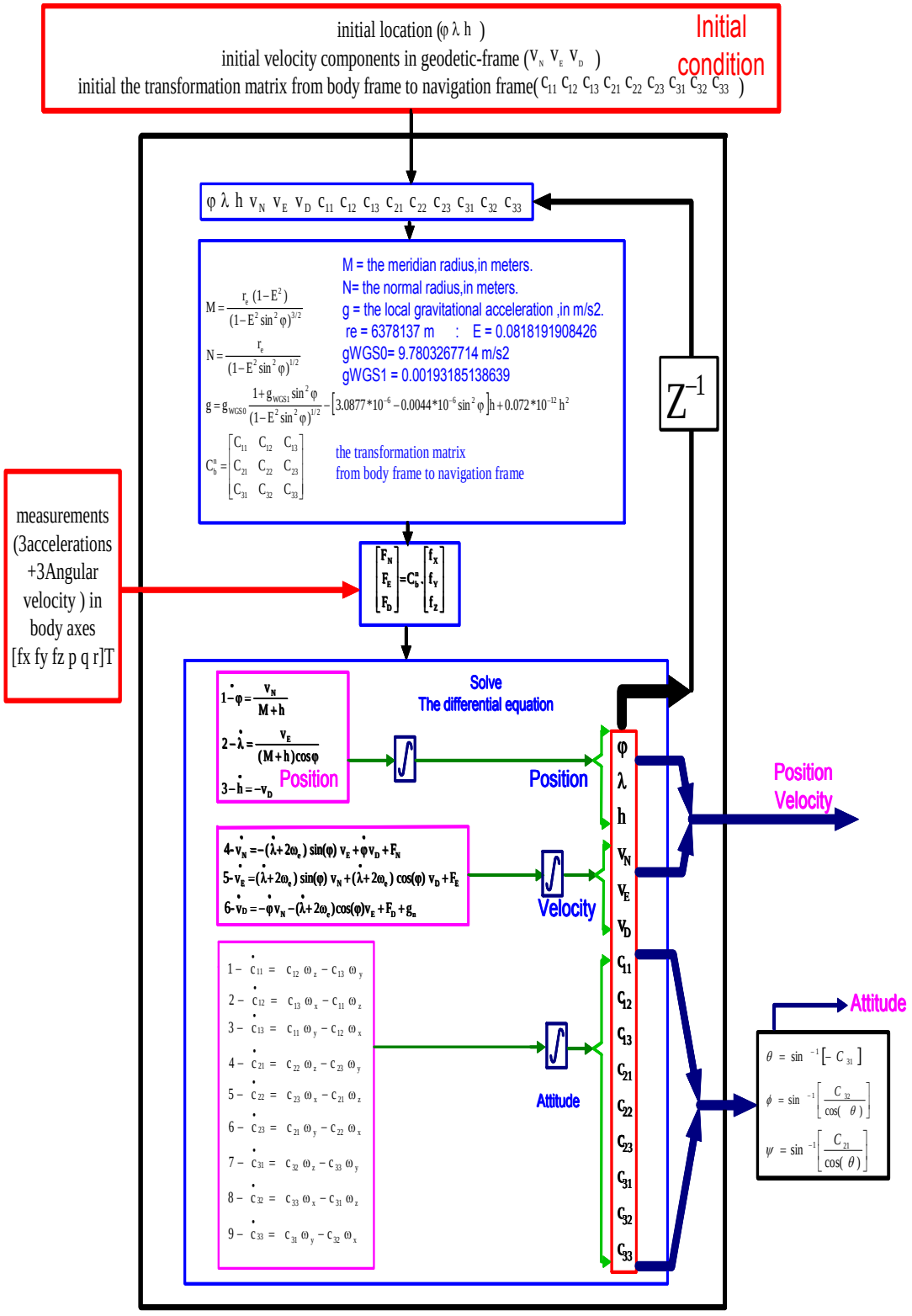

Fig.5: The flow chart of strapdown INS algorithm for attitude calculation based on direction cosines.

4.2.2 The Attitude Dynamics based on Direction Cosines using alternative Algorithm

$$\dot{C}_b^n = C_b^n \Omega_{nb}^b = C_b^n \left(\Omega_{ib}^b - \Omega_{in}^b\right) = \left(C_n^b\right)^T \quad (29)$$

or by [9]

$$\dot{C}_b^n = -\Omega_{nb}^b C_b^n \quad (30)$$

Where Ω represents the skew symmetric matrix forms of the vector ω and Ω_{ib}^b is the outputs of the strapdown gyroscopes. Ω_{bn}^n in Appendix A

$$\Omega_{nb}^b = -\begin{pmatrix} 0 & -c_{31}\omega_x - c_{32}\omega_y - c_{33}\omega_z & c_{21}\omega_x + c_{22}\omega_y + c_{23}\omega_z \\ c_{11}\omega_x + c_{12}\omega_y + c_{13}\omega_z & 0 & -c_{11}\omega_x - c_{12}\omega_y - c_{13}\omega_z \\ -c_{21}\omega_x - c_{22}\omega_y - c_{23}\omega_z & c_{11}\omega_x + c_{12}\omega_y + c_{13}\omega_z & 0 \end{pmatrix} \quad (31)$$

The Euler angles can also be determined from direction cosines by the following.

$$\theta = \sin^{-1}\left[-C_{31}\right] \quad (32)$$

$$\phi = \sin^{-1}\left[\frac{C_{32}}{\cos(\theta)}\right] \quad (33)$$

$$\psi = \sin^{-1}\left[\frac{C_{21}}{\cos(\theta)}\right] \quad (34)$$

The equations (3), (5), and (30) can be written in one equation form as given in equation (35).

$$\begin{pmatrix} \dot{r}^n \\ \dot{v}^n \\ \dot{C}_b^n \end{pmatrix} = \begin{pmatrix} D^{-1} v^n \\ C_b^n f^b - (2\omega_{ie}^n + \omega_{en}^n) \times v^n + g^n \\ -\Omega_{bn}^b C_b^n \end{pmatrix} \quad (35)$$

The flow chart, shown in Fig.6, indicates the details of strapdown INS algorithm for attitude calculation based on direction cosines (alternative Algorithm).

4.3 The Attitude Dynamics Using Quaternions

The Quaternions are used to rotate a vector from the NED frame to the BODY frame. Quaternions are singularity-free, have fewer issues with normalization, and trade bulky trigonometric functions with more convenient polynomial operations.

$$q_n^b = \begin{pmatrix} q_0 & q_1 & q_2 & q_3 \end{pmatrix}^T \quad (36)$$

The quaternions differential equation is:

$$\dot{q}_n^b = \frac{1}{2}\left(\Omega_{nb}^b\right) q_n^b \quad (37)$$

Where

$$\left(\Omega_{nb}^b\right) = \begin{pmatrix} 0 & -\omega_x & -\omega_y & -\omega_z \\ \omega_x & 0 & \omega_z & -\omega_y \\ \omega_y & -\omega_z & 0 & \omega_x \\ \omega_z & \omega_y & -\omega_x & 0 \end{pmatrix} \quad (38)$$

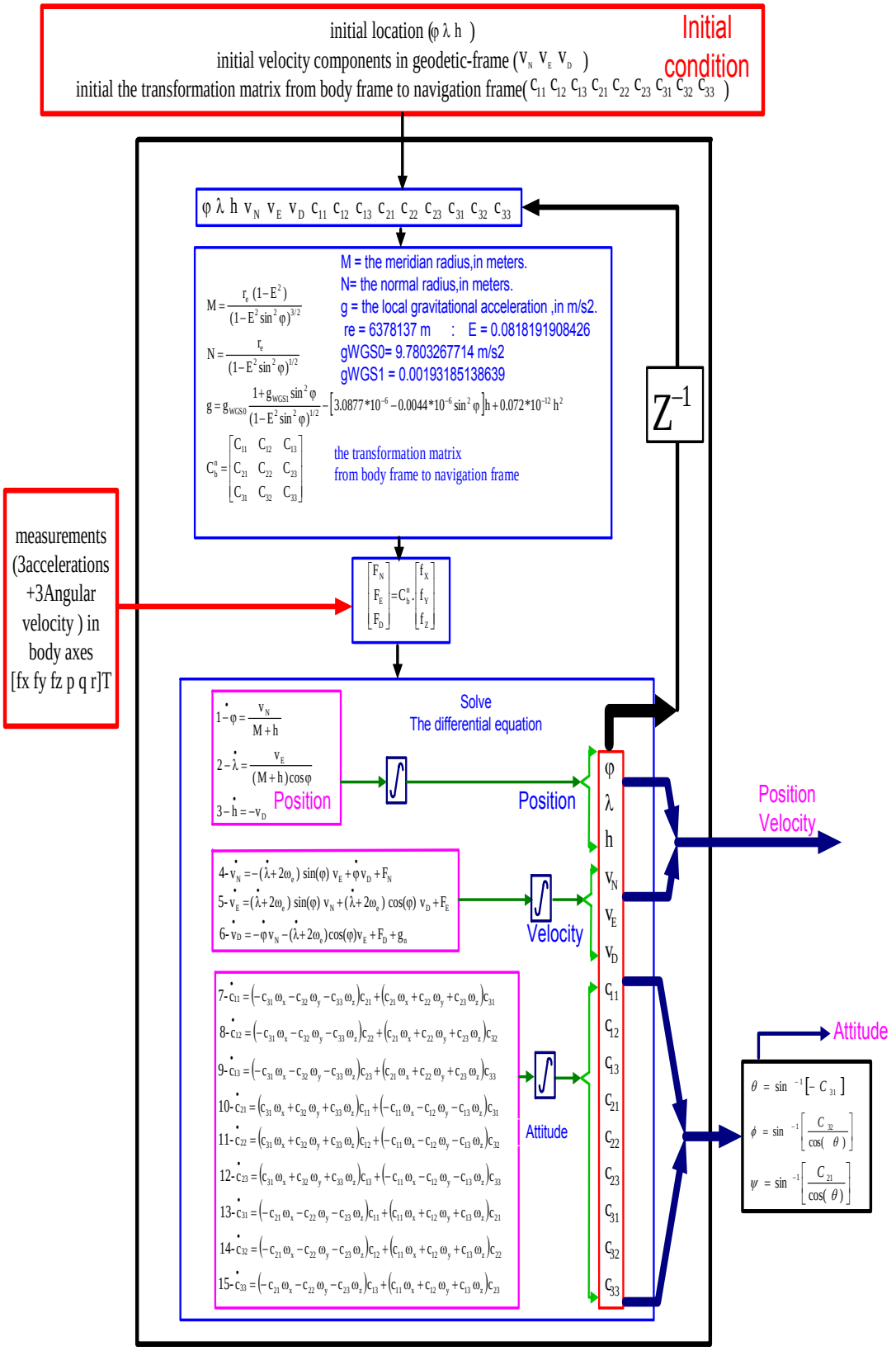

Fig.6: The flow chart of strapdown INS for attitude calculation based on direction cosines (alternative Algorithm).

The BODY frame is attached to the rate gyros, so the gyro signals measure the angular velocity of the BODY frame with respect to the inertial frame ω_{ib}^{b}. This can be decomposed into the angular velocities of the ECEF frame with respect to the ECI frame, ω_{ie}^{b}, the ECI frame with respect to the NED frame, ω_{en}^{b}, and the NED frame with respect to the BODY frame, ω_{nb}^{b}.

$$\omega_{ib}^{b} = \omega_{ie}^{b} + \omega_{en}^{b} + \omega_{nb}^{b} \tag{39}$$

Substituting equation (13) into the differential equation (11), we get:

$$\dot{q}_{n}^{b} = \frac{1}{2}\left(\Omega_{ib}^{b}\right) q_{n}^{b} - \frac{1}{2}\left(\Omega_{ie}^{b}\right) q_{n}^{b} - \frac{1}{2}\left(\Omega_{en}^{b}\right) q_{n}^{b} \tag{40}$$

The transformations between the quaternions and the DCM C_{b}^{n} are accomplished by [11].

$$C_{b}^{n} = \begin{pmatrix} q_1^2+q_0^2-q_2^2-q_3^2 & 2(q_1q_2+q_3q_0) & 2(q_1q_3-q_2q_0) \\ 2(q_1q_2-q_3q_0) & q_2^2+q_0^2-q_1^2-q_3^2 & 2(q_2q_3+q_1q_0) \\ 2(q_2q_3+q_2q_0) & 2(q_2q_3-q_1q_0) & q_3^2+q_0^2-q_1^2-q_2^2 \end{pmatrix}^{T} \tag{41}$$

The Euler angles can also be determined from quaternion by the following.

$$\theta = \sin^{-1}\left[-2(q_1q_3 - q_0q_2)\right] \tag{42}$$

$$\phi = \sin^{-1}\left[\frac{2(q_2q_3 + q_1q_0)}{\cos(\theta)}\right] \tag{43}$$

$$\psi = \sin^{-1}\left[\frac{2(q_1q_2 + q_3q_0)}{\cos(\theta)}\right] \tag{45}$$

The equations (3), (5), and (40) can be written in one equation form as given in equation (40).

$$\begin{pmatrix} \dot{r}^{n} \\ \dot{v}^{n} \\ \dot{q}_{n}^{b} \end{pmatrix} = \begin{pmatrix} D^{-1} v^{n} \\ C_{b}^{n} f^{b} - (2\omega_{ie}^{n} + \omega_{en}^{n}) \times v^{n} + g^{n} \\ \frac{1}{2}\left[\Omega_{ib}^{b}\right] q_{n}^{b} - \frac{1}{2}\left[\Omega_{ie}^{b}\right] q_{n}^{b} - \frac{1}{2}\left[\Omega_{en}^{b}\right] q_{n}^{b} \end{pmatrix} \tag{46}$$

The value of $\left(\Omega_{ie}^{b}\right) q_{n}^{b}$, and $\left(\Omega_{en}^{b}\right) q_{n}^{b}$ very small can be simplified equation (46). Because memes not sense these value

$$\begin{pmatrix} \dot{r}^{n} \\ \dot{v}^{n} \\ \dot{q}_{n}^{b} \end{pmatrix} = \begin{pmatrix} D^{-1} v^{n} \\ C_{b}^{n} f^{b} - (2\omega_{ie}^{n} + \omega_{en}^{n}) \times v^{n} + g^{n} \\ \frac{1}{2}\left[\Omega_{ib}^{b}\right] q_{n}^{b} \end{pmatrix} \tag{47}$$

The flow chart, shown in Fig.7, indicates the details of strapdown INS algorithm for attitude calculation based on quaternions.

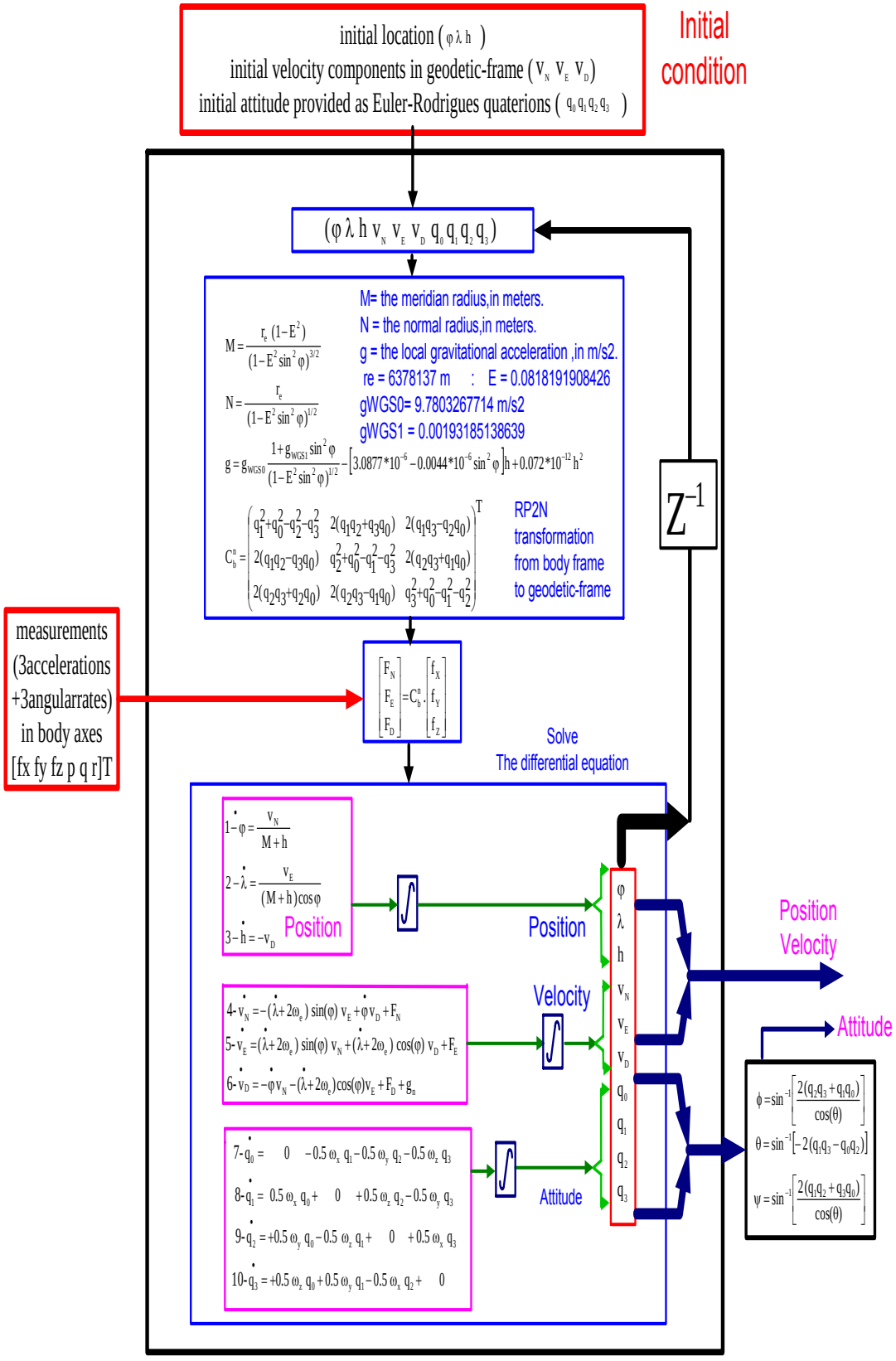

Fig.7: The flow chart of strapdown INS for attitude calculation based quaternions.

5-Simulation

Simulation of the proposed algorithms of strap down INS are based on Aircraft Model (Aerosonde UAV) given in [12]. Fig.8 shows AeroSim UAV in flight test.

Fig.8: Aerosonde UAV.

5.1 Aircraft Model

Simplified internal structure diagram Aircraft Model [12] (Aerosonde UAV) output position, velocity, and IMU measurement (acceleration, and Angular velocity). The model of Aircraft high fidelity because simulation of Aircraft The aerodynamics, propulsion, and inertia models compute the airframe loads (forces and moments) as functions of control inputs and environment (atmosphere and Earth) effects. The resulting accelerations are then integrated by the Equations of Motion to obtain the aircraft states (position, velocity, attitude, acceleration, angular velocities) show in Fig.9.

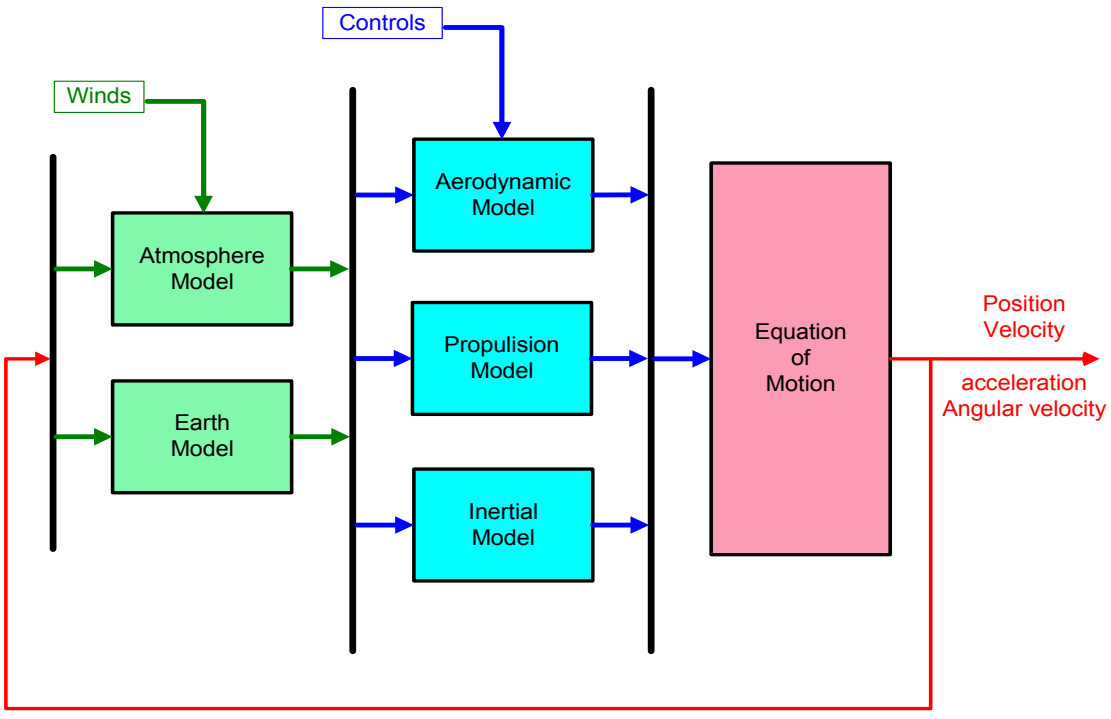

Fig.9: Simplified internal structure diagram Aircraft Model (Aerosonde UAV).

5.2 Simulation of IMU noise model

For simulation of the real IMU measurement (based on MEMS technology), the IMU noise model consists of Gyroscope Noise Model and Accelerometer Noise Model. The gyro measurement model [13] is given by the following equations.

$$\tilde{\omega}_{ib}^{b} = (I_{3\times3} + k_g)\,\omega_{ib}^{b} + b_g + \eta_{gv} \quad (48)$$

$$\dot{b}_g = \eta_{gu} \quad (49)$$

where b_g is the gyro "bias", k_g is a diagonal matrix of gyro scale factors, and η_{gv} and η_{gu} are zero-mean Gaussian white-noise processes with spectral densities given by $\sigma_{gv}^2 I_{3\times3}$ and $\sigma_{gu}^2 I_{3\times3}$, respectively.

The accelerometer measurement model [13] is given by the following equations.

$$\tilde{a}^{b} = (I_{3\times3} + k_a)\,a^{b} + b_a + \eta_{av} \quad (50)$$

$$\dot{b}_a = \eta_{au} \quad (51)$$

where b_a is the accelerometer "bias", k_a is a diagonal matrix of accelerometer scale factors, and η_{av} and η_{au} are zero-mean Gaussian white-noise processes with spectral densities given by $\sigma_{av}^2 I_{3\times3}$ and $\sigma_{au}^2 I_{3\times3}$ respectively.

A discrete-time simulation of gyro model using the spectral densities is shown in Fig.10, where $N = (0, \sigma^2)$ denotes a zero-mean normal distribution with σ^2 [13]. The same model can be used for the accelerometer measurements.

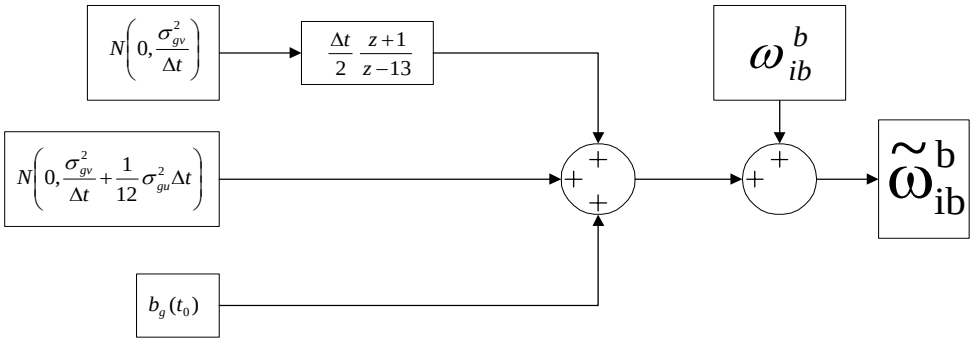

Fig.10: Gyroscope Noise Model.

The gyro noise parameters are given by

σ_{gv} =8.7266×10−7 rad/sec$^{1/2}$ and σ_{gu} = 9.1989×10−7 rad/sec$^{3/2}$.

The accelerometer parameters are given by

σ_{av} = 1.5 × 10−5 m/sec$^{3/2}$ and σ_{au} = 6 × 10−5 m/sec$^{5/2}$.

Initial biases for the gyros and accelerometers are given by

b_g =10 deg/hr and b_a =0.003 m/s^2.

5.3 Simulation Model Block Diagram

The simulation model block diagram contains fight control parameters (flap, elevator, aileron, rudder, throttle, mixture, and ignition). The INS algorithm is one of strapdown INS algorithms for attitude calculation (Euler angles, direction cosines, or quaternions). The difference between position velocity of Aircraft Model (Aerosonde UAV) and INS algorithm is considered as the error in position velocity as shown in Fig.11

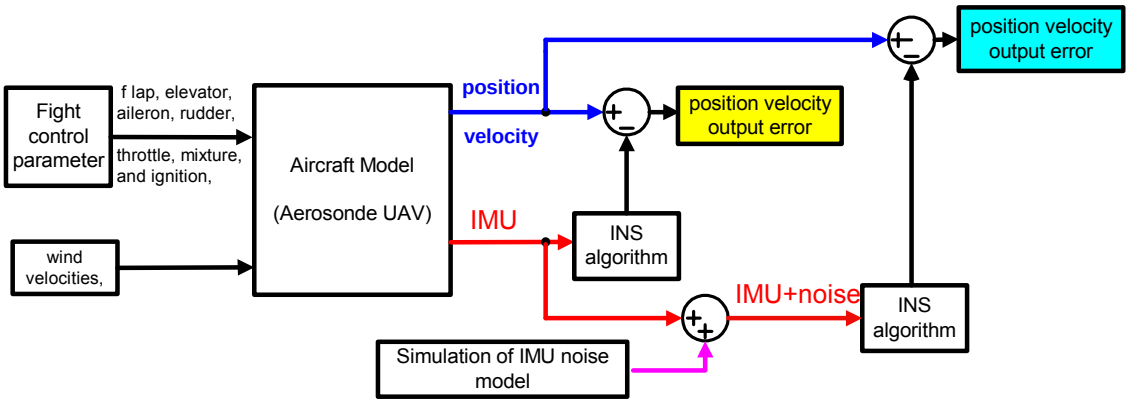

Fig.11: simulation model block diagram

5.4 Simulation Result

Run simulation with sampled time T_s= 0.01 seconds and the total time of the simulation is T= 300 seconds.

The position-velocity plot from of Aircraft Model (Aerosonde UAV) is considered as the real position-velocity. Fig.12. Shows the position in horizontal plan (navigation-frame), velocity in horizontal plan (navigation-frame), position [x, y, and z] in (navigation-frame) against time and velocity [x, y, and z] in (navigation-frame) against time

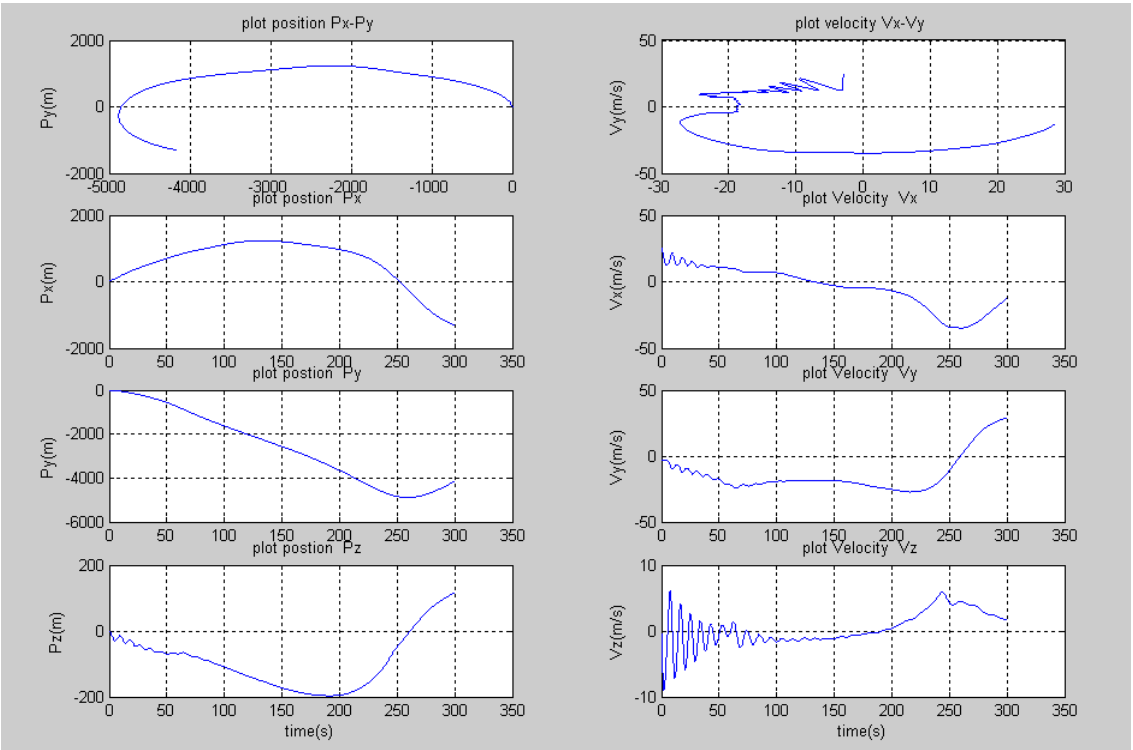

Fig.12: Position-velocity of Aerosonde UAV

The IMU output from the Aircraft Model (Aerosonde UAV) is considered as the real IMU measurement. The simulation of IMU MEMS measurement (noise model plus real IMU measurement) is shown in Fig.13 where specific force in body frame is

measured in m/sec^2 and angular velocity in body frame is measured in rad/sec.

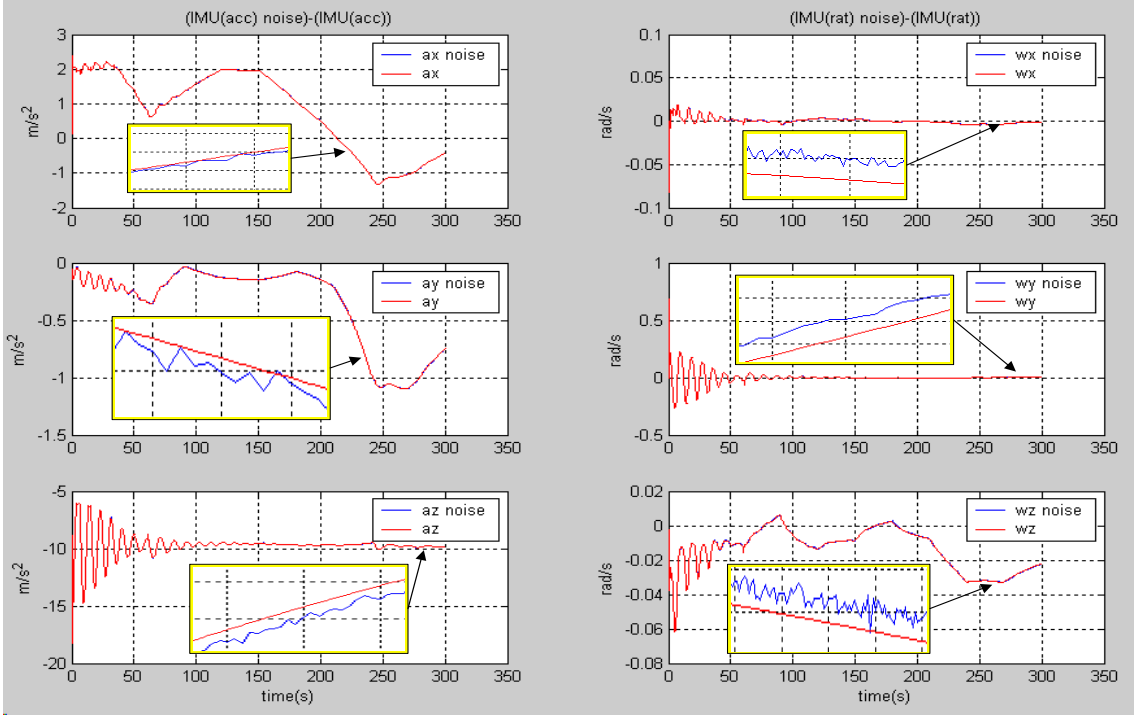

Fig.13 The simulation of IMU MEMS measurement

The rms error in position and velocity based on strapdown algorithms INS for attitude calculation (quaternions "INSQ", direction cosines "INSC2", direction cosines (alternative Algorithm) "INSC1", and Euler angles" INSE") are shown in Fig. 14

By taking the measurement data from IMU based on MEMS technology, the rms error in position and velocity using strapdown algorithms INS for attitude calculation are shown in Fig.15.

Taking the rms error of 10 runs with different IMU measurement noise (by changing the initial value of enhanced white noise added to the reading of IMU) and plot the error as in Fig. 15. As shown in Fig. 15 the minimum error in position in (x, y) and velocity (v_x, v_y) can be reached using the alternative method of direction cosines. In mean while we get the maximum rms error in position in (z) direction and in RMS error velocity in z direction (V_z).

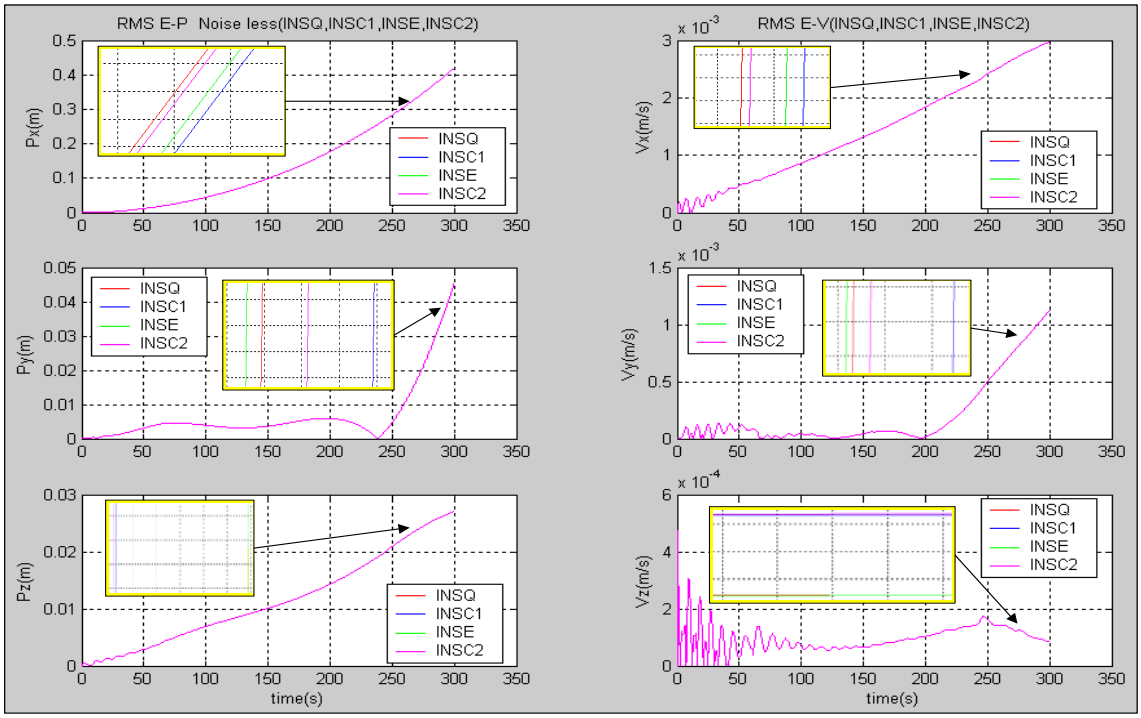

Fig.14 The rms error in position and velocity based on strapdown algorithms INS for attitude calculation.

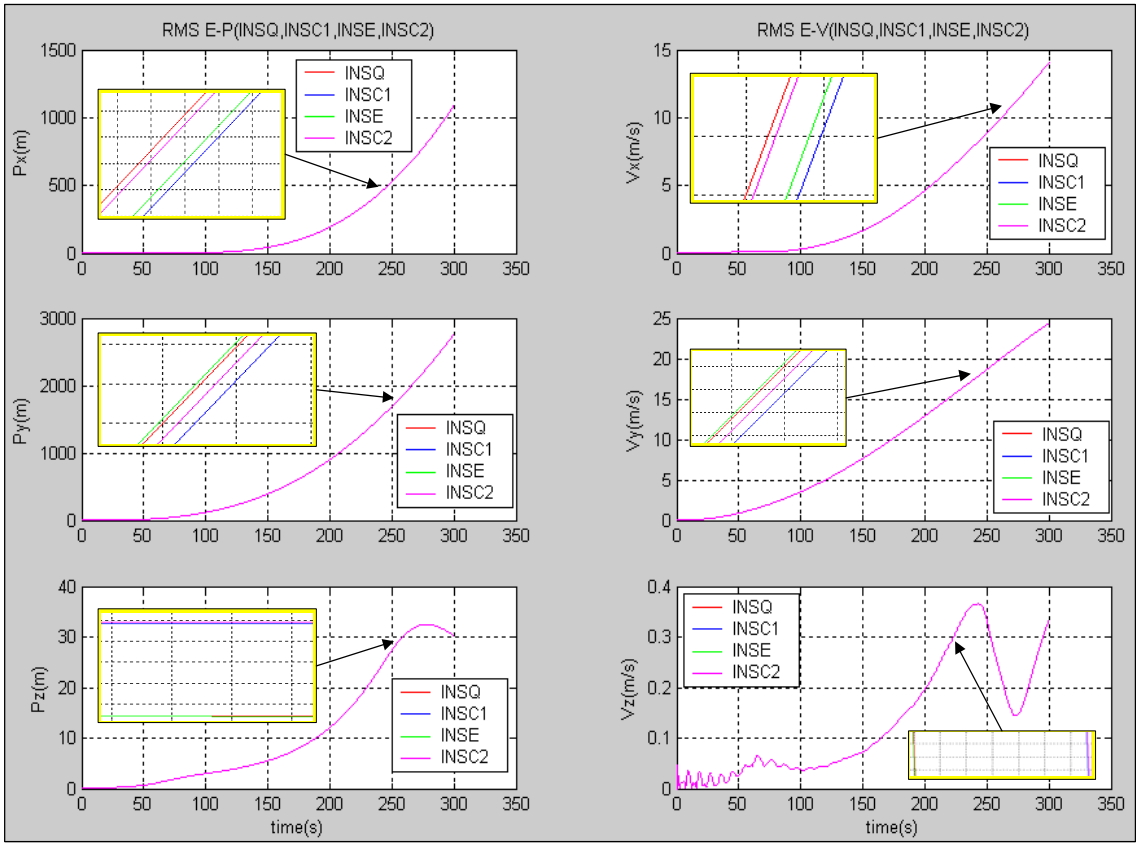

Fig.15 The rms error in position and velocity of 10 runs with different IMU measurement noise.

6 Comparisons of Different Types Strapdown INS Algorithms

Strapdown INS Algorithm	Advantage	Disadvantage
Euler angles	1- It has the lowest no. of equations parameters. 2-It has direct physical interpretation.	1- Solution of the differential equations suffer from singularities. 2-Euler angles are not directly derived from transformation matrix.
Direction cosines	1-Simple Model dynamic equations (linear differential equations). 2-Solution of the differential equations has no singularities.	1- Need to solve nine differential equations. 2-Euler angles are not directly derived from transformation matrix.
Direction cosines (alternative Algorithm)	1-Simple Model dynamic equations (linear differential equations). 2-Solution of the differential equations has no singularities. 3-Minumu rms error position and velocity in x,y coordinates.	1- Need to solve nine differential equations. 2- It has the highest of rms error in position and velocity in z direction. 3- Euler angles are not directly derived from transformation matrix. 4-More complex than direction cosines.
Quaternions	1- Easy to solve their dynamic equation. 2- Solution of the differential equations has no singularities. 3-More practical implementation in getting attitude variables in a strapdown navigation system. 4- Faster than other algorithms	1-It has less physical interpretation. 2-Transformation matrix and Euler angles are not directly derived from quaternions.

CONCLUSION

Simple reference flow charts of strapdown INS algorithms are introduced. An alternative algorithm for direction cosines is derived. Simulation of the proposed algorithms of strapdown INS is applied on the navigation system of Aircraft Model (Aerosonde UAV). Simulation results clarify that the strapdown INS algorithm using quaternions for attitude calculation is the most reliable algorithm. it is easy to solve its dynamic equations and its solution does not suffer from singularities. Moreover, it is faster than other algorithms. In the other hand, it dose not give lowest rms error in position and velocity.

Appendix A

$$\dot{C}_b^n = -\Omega_{nb}^n C_b^n \tag{b-1}$$

Where Ω represents the skew symmetric matrix forms of the vector w and Ω_{ib}^b is the outputs of the strapdown gyroscopes. Ω_{bn}^n is obtained by

$$\omega_{bn}^n = \omega_{in}^n - C_b^n \omega_{ib}^b \tag{b-2}$$

For the case where the quality of the gyroscope is so crude that we can disregard the Earth's rotation rate ω_{in}^n may be approximated by ω_{en}^n.

ω_{in}^n very small can simplifying ω_{en}^n

$$\omega_{bn}^n = -C_b^n \omega_{ib}^b \tag{b-3}$$

$$\omega_{bn}^n = \begin{pmatrix} -c_{11}\omega_x - c_{12}\omega_y - c_{13}\omega_z \\ -c_{21}\omega_x - c_{22}\omega_y - c_{23}\omega_z \\ -c_{31}\omega_x - c_{32}\omega_y - c_{33}\omega_z \end{pmatrix} \quad \begin{matrix} -c_{11}\omega_x - c_{12}\omega_y - c_{13}\omega_z \to \langle 1 \rangle \\ -c_{21}\omega_x - c_{22}\omega_y - c_{23}\omega_z \to \langle 2 \rangle \\ -c_{31}\omega_x - c_{32}\omega_y - c_{33}\omega_z \to \langle 3 \rangle \end{matrix} \tag{b-4}$$

$$-\Omega_{bn}^n = \left(\begin{array}{c|c|c} 0 & \langle 3 \rangle & -\langle 2 \rangle \\ \hline -\langle 3 \rangle & 0 & \langle 1 \rangle \\ \hline \langle 2 \rangle & -\langle 1 \rangle & 0 \end{array}\right) \tag{b-5}$$

$$\dot{C}_b^n = \begin{pmatrix} \dot{c}_{11} & \dot{c}_{12} & \dot{c}_{13} \\ \dot{c}_{21} & \dot{c}_{22} & \dot{c}_{23} \\ \dot{c}_{31} & \dot{c}_{32} & \dot{c}_{33} \end{pmatrix} = \left(\begin{array}{c|c|c} 0 & \langle 3 \rangle & -\langle 2 \rangle \\ \hline -\langle 3 \rangle & 0 & \langle 1 \rangle \\ \hline \langle 2 \rangle & -\langle 1 \rangle & 0 \end{array}\right) \begin{pmatrix} c_{11} & c_{12} & c_{13} \\ c_{21} & c_{22} & c_{23} \\ c_{31} & c_{32} & c_{33} \end{pmatrix} \tag{b-6}$$

$$\dot{c}_{11} = (-c_{31}\omega_x - c_{32}\omega_y - c_{33}\omega_z)c_{21} + (c_{21}\omega_x + c_{22}\omega_y + c_{23}\omega_z)c_{31} \tag{b-7}$$

$$\dot{c}_{12} = (-c_{31}\omega_x - c_{32}\omega_y - c_{33}\omega_z)c_{22} + (c_{21}\omega_x + c_{22}\omega_y + c_{23}\omega_z)c_{32} \tag{b-8}$$

$$\dot{c}_{13} = (-c_{31}\omega_x - c_{32}\omega_y - c_{33}\omega_z)c_{23} + (c_{21}\omega_x + c_{22}\omega_y + c_{23}\omega_z)c_{33} \tag{b-9}$$

$$\dot{c}_{21} = (c_{31}\omega_x + c_{32}\omega_y + c_{33}\omega_z)c_{11} + (-c_{11}\omega_x - c_{12}\omega_y - c_{13}\omega_z)c_{31} \tag{b-10}$$

$$\dot{c}_{22} = (c_{31}\omega_x + c_{32}\omega_y + c_{33}\omega_z)c_{12} + (-c_{11}\omega_x - c_{12}\omega_y - c_{13}\omega_z)c_{32} \tag{b-11}$$

$$\dot{c}_{23} = (c_{31}\omega_x + c_{32}\omega_y + c_{33}\omega_z)c_{13} + (-c_{11}\omega_x - c_{12}\omega_y - c_{13}\omega_z)c_{33} \tag{b-12}$$

$$\dot{c}_{31} = (-c_{21}\omega_x - c_{22}\omega_y - c_{23}\omega_z)c_{11} + (c_{11}\omega_x + c_{12}\omega_y + c_{13}\omega_z)c_{21} \tag{b-13}$$

$$\dot{c}_{32} = (-c_{21}\omega_x - c_{22}\omega_y - c_{23}\omega_z)c_{12} + (c_{11}\omega_x + c_{12}\omega_y + c_{13}\omega_z)c_{22} \tag{b-14}$$

$$\dot{c}_{33} = (-c_{21}\omega_x - c_{22}\omega_y - c_{23}\omega_z)c_{13} + (c_{11}\omega_x + c_{12}\omega_y + c_{13}\omega_z)c_{23} \tag{b-15}$$

REFERENCES

[1] Savage P. G "Strapdown inertial navigation integration algorithm design part 1: Attitude algorithms" Journal of Guidance Control and Dynamics, vol. 21, NO. 1, pp. 19-28, January-February, (1998).
[2] Savage P. G "Strapdown inertial navigation integration algorithm design part 2: Velocity and position" Journal of Guidance Control and Dynamics, vol. 21, NO. 2, pp. 208-221, March-April , (1998).
[3] Grewal M. S. Weill L. R. and Andrews A. P., Global Positioning Systems Inertial Navigationand Integration. New York: John Wiley and Sons Inc, (2001).
[4] Rogers R. M. Applied Mathematics in Integrated Navigation Systems. American Institute of Aeronautics and Astronautics Inc, (2000).
[5] Friedland, B. "Analysis Strapdown Navigation Using Quaternions" IEEE Transitions on Aerospaceand Electronic System, vol. AES-14, NO. 5, pp. 764-768, September, (1978).
[6] George M. Siouris. Aerospace Avionics Systems. New York: Academic Peress, INS, (1993).
[7] D.H. Titterton and J. L. Weston . Strapdown inertial navigation technology. London, U.K.: Peter Peregrinus Ltd, (1997).
[8] Xiaohong Zhang. Integration of GPS with Medium Accuracy IMU Meter-Level Position. Msc. Thesis, The University of Calgary, Alberta, May, (2003).
[9] Eun-Hwan Shin. Accuracy Improvement of Low Cost INS/GPS for Land Applications. Msc. Thesis, The University of Calgary, Alberta, December, (2001).
[10] Litmanovich, Y. A., Lesyuchevsky, V. M., and Gusinsky, V. Z. "Two new classes of strapdown navigation algorithms" Journal of Guidance Control and Dynamics, vol. 23, NO. 1, pp. 34–44, January-February, (2000).
[11] Anthony Kim. Development of Sensor Fusion Algorithms for MEMS-Based Strapdown Inertial Navigation Systems . Msc. Thesis, the University of Waterloo, Ontario, Canada, (2004).
[12] AeroSim aeronautical simulation blockset Version 1.1,
http://www.u dynamics.com.
[13] Jasbir Singh Vig . IMPROVED NAVIGATION OF A VEHICLE USING INS/GPS WITH LINE OF SIGHT MEASUREMENTS. Msc. Thesis, The State University of New York at Buffalo, September 1, (2005).